Nonlinear Waves in Film Viscous Liquid Flows at Arbitrary Kapitsa Numbers

A. N. Beloglazkin[a,*] and V. Ya. Shkadov[a,**]

[a]Moscow State University, Moscow, Russia

*e-mail: bel@mech.math.msu.su

**e-mail: shkadov@mech.math.msu.su

Abstract—The methods and results of the mathematical simulation of nonlinear waves generated by hydrodynamic instability in traveling capillary films of a viscous liquid are discussed. Two model systems of differential equations for the local values of the layer thickness h and the fluid flow rate q are considered. The single-parameter $(h-q)$ Kapitsa–Shkadov model that ensures the effective simulation of low-viscosity liquid film flows has received wide acceptance in world literature devoted to film hydrodynamics. The two-parameter $(h-q)_1$ model extends the possibilities for direct calculation of nonlinear waves in the higher viscosity liquid films. A succession of the systems of model equations is given, the scenarios of instability and bifurcation are discussed, and the results of calculations of wave structures in comparison with the experimental data are given.

In the present study, the wave regimes of film flows of viscous liquids in which the viscosity coefficients vary within wide limits are considered. An approximate model system of differential equations with two external governing parameters for the layer thickness and the local fluid flow rate [1] is used. This system takes more precisely into account viscous dissipation in the layer as compared with the well-known single-parameter Shkadov model [2]. New properties of linear and nonlinear waves generated by hydrodynamic instability of flows of highly viscous liquids under the action of the gravity force and the surface tension are discussed.

The basic property of the two-parameter system consists in existence of a curve in the plane of governing parameters which separates the set of regular wave solutions in two subsets. In the first case a series of bifurcations of slow waves from the neutral curve takes place and only thereafter transition to the family of fast waves occurs. In the second case there is a single bifurcation of the family of fast waves from the basis state on the neutral curve and the fast waves are immediately formed.

1. MODEL EQUATIONS OF WAVE FILM FLOWS

Flow of thin layers of viscous liquid along a solid surface under the action of the gravity, viscosity, and surface tension forces can be described by the boundary value problem [2] which includes the Navier–Stokes equations

$$u_t + uu_x + vu_y = -p_x + \frac{1}{\kappa \text{Re}}(u_{yy} + \kappa^2 u_{xx}) + \frac{1}{\kappa \text{Fr}},$$

$$v_t + uv_x + vv_y = -\frac{2}{\kappa \text{Re}}p_{1y} + \frac{1}{\kappa \text{Re}}(v_{yy} + \kappa^2 v_{xx}),$$

$$u_x + v_y = 0,$$

$$p = \frac{2\kappa}{\text{Re}}p_1 - \frac{\kappa^2}{\text{We}}\frac{h_{xx}}{(1 + b^2)^{3/2}}, \quad b = \kappa h_x$$

(1.1)

and the boundary conditions

$$y = 0: \quad u = 0, \quad v = 0,$$

$$y = h : \begin{cases} p_1 = \dfrac{1+b^2}{1-b^2} v_y \\[2mm] u_y + \kappa^2\left(v_x + \dfrac{4h_x}{1+b^2} v_y\right) = 0 \\[2mm] h_t + uh_x = v. \end{cases} \tag{1.2}$$

Equations (1.1) and (1.2) are written in dimensionless form. The subscript denotes the partial derivative with respect to the corresponding variables. The length scales h_0 and $\dfrac{h_0}{\kappa}$ are used for the variables y and x, the velocity scales U_0 and κU_0 are used for the velocities u and v, and the dynamic pressure ρU_0^2 is used for the pressures p and p_1. The characteristic values of the layer thickness h_0 and the liquid velocity U_0, as well as the coefficient κ of extension along the streamwise variable x must be additionally specified.

The boundary-value problem (1.1), (1.2) contains following dimensionless parameters: the Reynolds number $\mathrm{Re} = \dfrac{U_0 h_0}{\nu}$, the Weber number $\mathrm{We} = \dfrac{\rho h_0 U_0^2}{\sigma}$, and the Froude number $\mathrm{Fr} = \dfrac{U_0^2}{g h_0}$. We will consider only the gravity-capillary flows of viscous incompressible liquids in which the viscosity, gravity, and surface tension forces are of the same order given by the quantity δ in accordance with the relations [2, 3]

$$\frac{\kappa^2}{\mathrm{We}} = \frac{3}{\kappa \mathrm{Re}} = \frac{1}{\kappa \mathrm{Fr}} = \frac{1}{5\delta}. \tag{1.3}$$

Hence we can find the dimensionless criteria and the scaling factors h_0 and U_0 characteristic of the flow class considered:

$$\mathrm{We} = 5\delta\kappa^2, \quad \mathrm{Re} = \frac{15\delta}{\kappa}, \quad \mathrm{Fr} = \frac{5\delta}{\kappa} \quad h_0 = \left(3\mathrm{Re}\,\frac{\nu^2}{g}\right)^{1/3}, \quad U_0 = \frac{g h_0^2}{3\nu}. \tag{1.4}$$

Now, the problem (1.1), (1.2) is completely determined by the pair of external governing parameters of the mathematical model δ and κ.

In [4, 5] the significance of scaling (1.3) and introduction of the parameter δ for successful solution of the problem of nonlinear waves in films was noted.

In [1] derivation of the following model system of equations was given

$$h_t + q_x = 0,$$

$$q_t + \frac{6}{5}\left(\frac{q^2}{h}\right)_x = \frac{1}{5\delta}\left(h - \frac{q}{h^2} + hh_{xxx}\right)$$

$$+ \frac{\kappa^2}{5\delta}\left(\frac{5}{3}q_{xx} - \frac{9}{4}\frac{qh_{xx}}{h} - \frac{3}{2}\frac{q_x h_x}{h} + \frac{3}{2}\frac{qh_x^2}{h^2}\right). \tag{1.5}$$

The terms on the right-hand side of (1.5) with the multiplier κ^2 reflect more exact account of the effect of viscosity in the initial boundary-value problem (1.1), (1.2). For small κ, neglecting the terms with the multiplier κ^2, from (1.5) we can obtain the model $(h - q)$ system derived in [2]. For large γ (low viscosity) this system is controlled by a single parameter δ and can be reduced to the form:

$$h_t + q_x = 0,$$

$$q_t + \frac{6}{5}\left(\frac{q^2}{h}\right)_x = \frac{1}{5\delta}\left(h - \frac{q}{h^2} + hh_{xxx}\right). \tag{1.6}$$

The system (1.6) was the base of the integral method for calculating nonlinear waves in films of low-viscosity liquid in the long series of studies cited in [4, 6]. The complete $(h - q)_1$ system (1.5) contains two external parameters δ and κ and is destined for investigation of waves in liquids with an arbitrary viscosity.

Table 1. Values of γ and κ for $\delta = 0.15$

γ	3750	1323	102.9	23.25	8.1	3.572
κ	0.15	0.2	0.4	0.6	0.8	1.0

In [7, 8] the history of constructing the system of Shkadov evolutionary equations (1.6) was outlined starting from the instant of its creation in 1967 [2], and it was given its partial asymptotic case, namely, the weakly nonlinear equation of the integral method of theory of wave films, first derived in [2] and investigated in [7]

$$H_t + (3H^2 - cH + H_x + H_{xxx})_x = 0. \tag{1.7}$$

The investigation of this equation was continued and first published in form (1.7) in [9] with the following remark: "note that the equation of form (1.7) can be also obtained from equations derived in [2], if only the principal terms in k_m are conserved in these equations." A fairly detailed investigation of wave solutions of the weakly nonlinear equation (1.7) was carried out in [10].

Equation (1.7) represents asymptotic form of the model system (1.6), as the flow rate tends to zero. For finite values of δ the system (1.6) describes the physical waves which can be compared with experiments. Asymptotic equation (1.7) corresponds to the mathematical waves of infinite length and infinitely small amplitude and it does not contain any parameters that can be related to the experimental conditions. Note that the mathematical model of unsteady nonlinear waves in films can be reduced to a single equation only under as $\delta \to 0$. For finite values of δ unsteady wave film flows can be described by the system of two equations (1.6).

The useful application of the weakly nonlinear equation of theory of falling wave films (1.7), which is limiting as $\delta \to 0$, is connected with the possibility of using its solutions for calculation of the initial data in iterative computations at $\delta \neq 0$. This approach was used in [11] for numerical solution of system (1.6) and in [1] for calculation of the solutions of system (1.5).

We note that some attempts to supplement the $(h - q)$ model with terms quadratic in the wavenumber α were undertaken in [12, 13], while in [14] modifications of the $(h - q)$ system (1.6) by introducing the weight coefficients in integrating the first of the equations (1.1) with respect to y were considered.

The problem (1.5) is determined by the pair of external governing parameters of the mathematical model: δ and κ. In the experimental studies the parameters $R = 3\text{Re}$ and $\gamma = \dfrac{\sigma}{\rho}(\nu^4 g)^{-1/3}$ are frequently used. According to (1.4), these parameters are connected with δ and κ by the relations:

$$\delta = \frac{R^{11/9}}{45\gamma^{1/3}}, \quad \kappa = \frac{R^{2/9}}{\gamma^{1/3}}, \quad R = \frac{45\delta}{\kappa}, \quad \gamma = \frac{(45\delta)^{2/3}}{\kappa^{11/3}}. \tag{1.8}$$

In Fig. 1 we have reproduced the domains of governing parameters in the (R, γ) and (δ, κ) planes at which the experiments on wave films were carried out. Curves *1* and *2* bound the domain *A* of large values of γ that correspond to low-viscosity liquids. This includes the classic experiments of [15] and many other successive studies whose results were collected in [16]. Curve $\kappa = 0.2$ passes through the central part of this domain; therefore, in solving the problem (1.1), (1.2) we can adopt the assumption $\kappa^2 \ll 1$. In [2, 3] the corresponding theory including derivation of the approximate model $(h - q)$ problem with a single external governing parameter δ and investigation of solutions for periodic and solitary waves was constructed. This theory made it possible to interpret the experimental results, it obtained the further development and generalization by taking the processes of heat- and mass-exchange in films into account and is successively used to present time [6].

Curves *3* and *4* bound the vast domain *B* of new experiments [12, 13] with wave film flows at large and small values of γ. It can be seen that the inequalities $0.1 < \kappa < 1$ hold for the indicated set of experimental points, the values of κ increasing with decrease in γ. In Table 1, as an example, we have given the values of γ and κ for $\delta = 0.15$. As the viscosity increases, γ decreases and κ grows, reaching the value $\kappa \sim 1$ ($\kappa = 0.15$ for $\gamma = 3750$ and $\kappa = 1$ for $\gamma = 3.572$). The domain of small γ is of particular interest for the higher viscosity liquids. In this domain the waves are not sufficiently studied and it is necessary both to develop theory and to carry out new detailed calculations.
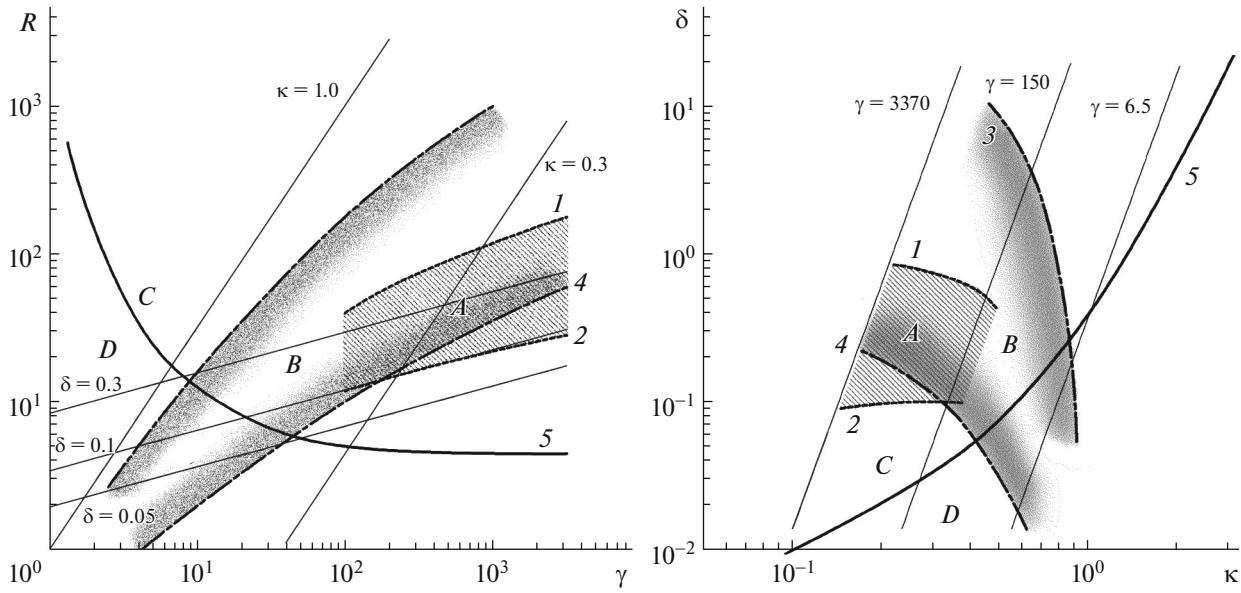
Fig. 1. Domains of existence of the wave film flow regimes in the (R, γ) and (δ, κ) planes: curves *1* and *2* correspond to curves bounded the domain *A* that corresponds to low-viscosity liquids; curves *3* and *4* correspond to curves bounded the domain *B* of wave film flows at large and small γ; curve *5* corresponds to bifurcation saddle-point that separates the domains *C* and *D*.

2. BIFURCATION BARRIER

The basic state of system (1.5) corresponds to dynamically possible flow of film of constant thickness and constant flow rate $h = 1$ and $q = 1$. We will consider the conditions under which, as a result of hydrodynamic instability, soft bifurcation from the basic state of the wave flow regime with the wavenumber α takes place

$$h = 1 + \hat{h} \exp i\alpha(x - ct), \quad q = 1 + \hat{q} \exp i\alpha(x - ct).$$

Linearizing system (1.5) with respect to low amplitudes $\hat{h}$ and $\hat{q}$, we obtain the following dispersion relation for determining the eigenvalue $c = c(\alpha, \delta, \kappa^2)$ in the instability domain $0 < \alpha \leq \alpha_n$

$$c^2 - \frac{12}{5}c + \frac{6}{5} + \frac{i}{5\alpha\delta}(c - 3) - \frac{\alpha^2}{5\delta} + \frac{i\alpha\kappa^2}{5\delta}\left(\frac{5}{3}c - \frac{9}{4}\right) = 0. \tag{2.1}$$

Setting $c_i = 0$ in (2.1), we can derive the equations for α_n and c_r on the neutral curve

$$c_r - 3 + \alpha_n^2 \kappa^2 \left(\frac{5}{3}c_r - \frac{9}{4}\right) = 0,$$

$$\alpha_n^2 = 5\delta\left(c_r^2 - \frac{12}{5}c_r + \frac{6}{5}\right). \tag{2.2}$$

We will calculate $\dfrac{dc_r}{d\alpha}$ for the dispersion relation (2.1) at points of the neutral curve. From the condition $\dfrac{dc_r}{d\alpha} = 0$ we obtain

$$\frac{\kappa^4}{\delta} = \frac{24}{11}\frac{(3 - c_r)(c_r - 1.2)}{c_r - 1.35}. \tag{2.3}$$

In Fig. 1 curve *5* represents the set of points in the (κ, δ) plane at which the relations (2.2) and (2.3) are simultaneously fulfilled. At each point of the domain *C* (above curve *5*) the condition $\dfrac{dc_r}{d\alpha} > 0$ is fulfilled

Table 2. Bifurcation saddle-points

γ	1.588	2.479	4.437	10.37	41.41	354.9	4141
R	328.9	95.88	30.34	11.27	5.769	4.671	4.552
κ	3.107	2.037	1.300	0.7854	0.4267	0.1989	0.0873
δ	22.71	4.340	0.8757	0.1966	0.0547	0.0207	0.0088

on the neutral curve and the condition $\dfrac{dc_r}{d\alpha} < 0$ is fulfilled at each point in the domain D. Change in sign of $\dfrac{dc_r}{d\alpha}$ leads to a modification of the character of soft bifurcation of the wave regime. The soft bifurcation takes place in the neighborhood of neutral curve when α is displaced to the instability domain $\alpha = \alpha_n + \delta\alpha$, $\delta\alpha < 0$. Consequently, slow waves with the phase velocity lower than the phase velocity of neutral waves $c_r < c_{rn}$ softly branch off in the domain C on the neutral curve. Correspondingly, fast waves with the phase velocity $c_r > c_{rn}$ softly branch off in the domain C on the neutral curve. Curve 5 represents a bifurcation saddle-point curve which separates the film flows of type I in the domain C and of type II in the domain D.

The family of slow waves γ_1 branches off on the neutral curve $\alpha = \alpha_n$ in flows of type I at fairly large γ. As the wavenumber decreases, a critical value of $\alpha = \alpha_*$ is reached. At such an α rigid bifurcation of the family of fast waves γ_2 takes place. This continues with variation in the inner parameter α to the point $\alpha = 0$.

Bifurcations of the first family γ_1 disappear in transition across the bifurcation saddle-point curve into the domain D to flows of the type II. The family of fast waves γ_2 branches off at once on the neutral curve. This family continues with variation in the inner parameter α to the point $\alpha = 0$.

In [11] the concept of slow and fast waves with inner parameter α at small δ was first introduced. In [11] the basic principal properties of regular waves at finite δ were also formulated. Thereafter, it was shown [17] that for $\delta > 0.09$ rigid bifurcations of intermediate families of slow waves develop. Their number increases with δ. Accordingly, the point of rigid bifurcation of the family γ_2 is displaced towards small α.

In Fig. 1 bifurcation saddle-point curve 5 divides the set of experimental points [13] into two large groups in the (κ, δ) plane. For them the properties of nonlinear waves initiated by hydrodynamic instability are significantly different, but the wave solutions of the $(h - q)_1$ system correspond to those and that one. In Table 2 we have represented certain values of the governing parameters for the points located on the bifurcation saddle-point curve.

3. REGULAR PERIODIC WAVES

In the case of spatially-periodic waves, for each pair of external independent parameters R and γ (or δ and κ) there also exists an inner parameter, namely, a wavenumber α such that for $0 < \alpha \le \alpha_n$ small perturbations are unstable and develop into nonlinear regular waves, and α_n is a point on the neutral curve. As α varies from the point $\alpha = \alpha_n$ to the point $\alpha = 0$, the character of wave solutions (1.5) changes from harmonic waves (slow or fast) to fast solitary waves—solitons. In [1] the fundamental property of system (1.5) was established. In the plane of governing parameters there exists a curve (curve 5 in Fig. 1) that separates the set of regular wave solutions into two subsets, namely, in the domain A slow waves (the phase velocity c_r is lower than the phase velocity of neutral waves) branch off from steady-state flow at each point of any neutral curve, while in the domain B fast waves branch off. In Fig. 1b straight lines $\gamma = $ const intersect the bifurcation saddle-point curve 5 [1], the point of intersection depending on γ. With decrease in κ the structure of wave solutions is modified in transition through the point of intersection, in particular, fine-scale ripples disappear on the leading wave front. In what follows, we will give the results of direct numerical solution of the two-parameter model for periodic and solitary waves.

In the general case, for an arbitrary shape of the liquid film surface the solutions were found numerically by the method of establishing in time with the use of the Fourier representations in the spatial variable x:

$$h(t, x) = \sum_{n=-\infty}^{\infty} h_n(t) \exp i\alpha nx, \quad q(t, x) = \sum_{n=-\infty}^{\infty} q_n(t) \exp i\alpha nx. \tag{3.1}$$
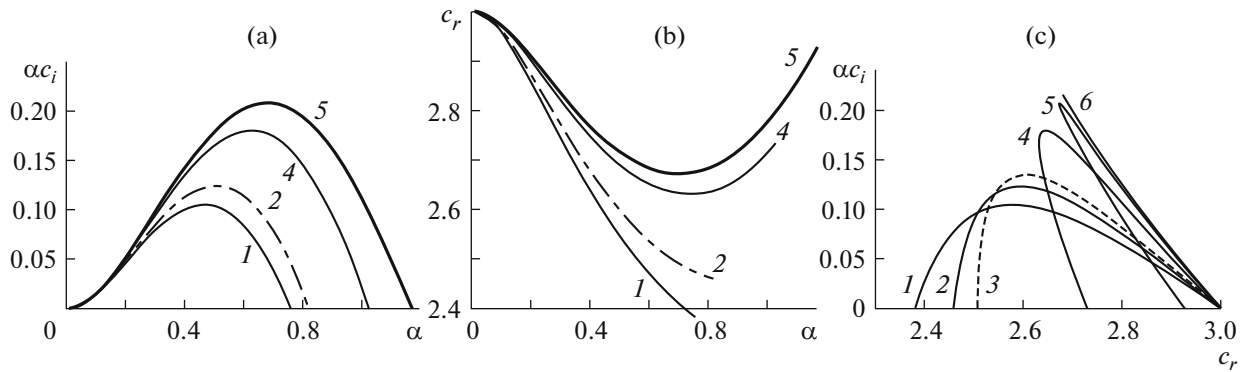
Fig. 2. Dependence of the growth rate coefficient αc_i and the phase velocity c_r in the domain of linear instability for $\delta = 0.1$ and various values of γ: 6.5 (curve *1*), 12.6 (curve *2*), 19 (curve *3*), 150 (curve *4*), 3370 (curve *5*), and ∞ (curve *6*).

Substituting (3.1) in (1.5), we obtain the corresponding dynamical system of nonlinear ordinary differential equations for the expansion coefficients $h_n(t)$ and $q_n(t)$ which can be numerically integrated in time using the direct and inverse Fourier transforms. As the initial conditions for the coefficients h_0 and q_0, we specified the values for undisturbed stream and small values for h_1 and q_1 were used as the initial perturbations.

For periodic waves with the wavelength $2\pi/\alpha$ we used the following boundary conditions:

$$h(0) = h(2\pi/\alpha), \quad h_x(0) = h_x(2\pi/\alpha), \quad h_{xx}(0) = h_{xx}(2\pi/\alpha). \tag{3.2}$$

For each calculation we specified values of the governing parameters δ, κ, and α (or R, γ, and α).

In Fig. 2a and 2b we have reproduced the growth rate coefficient αc_i and the phase velocity c_r as functions of the wavenumber α obtained from an analysis of the linearized problem. The results are represented for various γ in the case of α from the instability interval. For large values of $\gamma = 3370$ and 150 bifurcation occurs from the neutral curve initially to slow waves and only thereafter transition to fast waves takes place. For smaller $\gamma = 12.6$ and 6.5 fast waves are formed at once. In Fig. 2c we have plotted the graphs of the growth rate coefficient αc_i as a function of the phase velocity c_r for various γ. The condition $\left.\dfrac{d\alpha c_i}{dc_r}\right|_{\alpha_0} = \infty$ is fulfilled for $\gamma \approx 19$. For the greater values of γ the dependence of the growth rate coefficient αc_i on the phase velocity c_r is not single-valued: the value of α at which the condition $\dfrac{d\alpha c_i}{dc_r} = \infty$ is fulfilled is located inside the instability interval and for a single phase velocity c_r there exist two different values of the growth rate coefficient αc_i in the interval $\alpha_{max} < \alpha < \alpha_0$, where α_{max} is the wavenumber for the maximum growth rate coefficient αc_i and α_0 is the wavenumber of neutral oscillations. As $\gamma \to 0$, $c_r(\alpha_0) \to 3$. Then we obtain the case (*6*) in which each point of the curve corresponds to two different values of α from the interval of linear instability.

As $t \to \infty$, when $\alpha = $ const is fixed, the limiting solutions of the system of evolutionary equations represent dominating waves. For each given δ the set of dominating waves from the instability interval $(0 < \alpha < \alpha_n)$ forms a global attractor [6].

In Fig. 3, in which the results of direct numerical solution of system (1.5) for limiting waves of the global attractor are shown for the domains C and D for $\delta = 0.1$ (curves *1* and *2* correspond to $\gamma = 3370$ and $\gamma = 6.5$, respectively), we can see the differences between the scenarios of bifurcations in flows of types I and II. In the first case there is a series of bifurcations of slow waves before transition to the family of fast waves γ_2, the local maxima on curves $q_0 = q_0(\alpha)$ and $c_r = c_r(\alpha)$ correspond to them; in the second case there is a single bifurcation of the family of fast waves γ_2 from the basis state on neutral curve at $\alpha = \alpha_n$.

In Fig. 4 we have illustrated the range of variation in the phase velocity c_r for a highly viscous liquid. Here, we have shown the dependence of c_r on the reduced maximum film thickness $h_{max} - 1$ in the case of
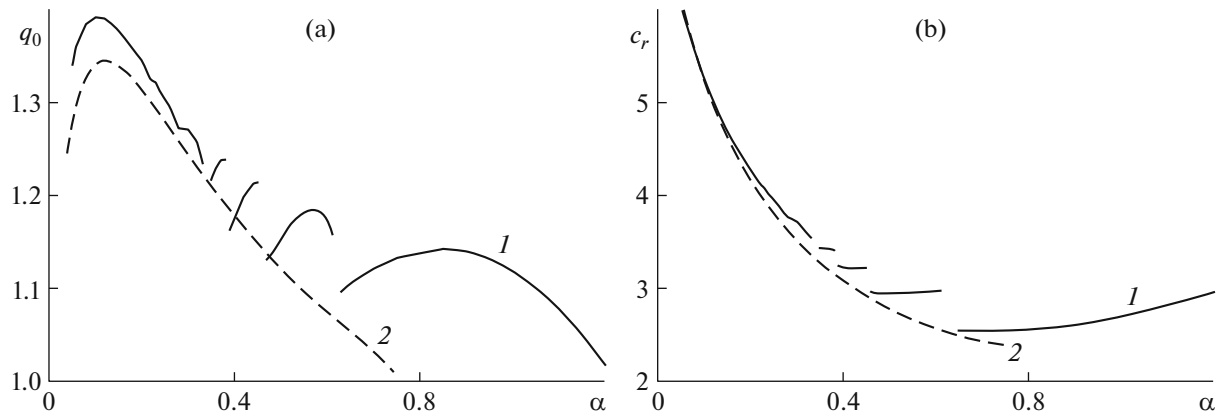
Fig. 3. Global attractor at $\delta = 0.1$: (a) projection to the (q_0, α) plane; (b) projection to the (c_r, α) plane; curves *1* correspond to $\gamma = 3370$ and curves *2* correspond to $\gamma = 6.5$.
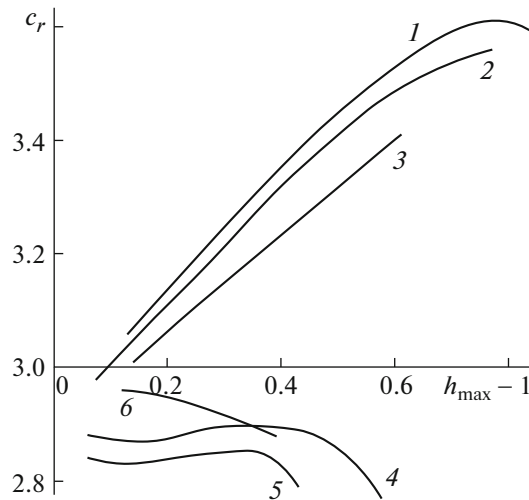

Fig. 4. Dependence of the phase velocity c_r on the reduced maximum film thickness $h_{max} - 1$ in the case of $\alpha = 0.15$ (curves *1*, *2*, and *3* correspond to $\gamma = 22$, 13, and 6.5, respectively) and for $\alpha = \alpha_m$ that corresponds to the maximum growth rate coefficient αc_i (curve *4* corresponds to $\gamma = 22$, curve *5* to 13, and curve *6* to 6.5).

$\alpha = 0.15$, $\gamma = 22$ (curve *1*), $\gamma = 13$ (curve *2*), $\gamma = 6.5$ (curve *3*) and at $\alpha = \alpha_m$, where α_m corresponds to the maximum growth rate coefficient αc_i, $\gamma = 22$ (curve *4*), $\gamma = 13$ (curve *5*), and $\gamma = 6.5$ (curve *6*).

For $\kappa^2 \ll 1$ the wave solutions of the model $(h - q)$ system of study [2] are characterized by the presence of capillary ripples on the leading front of fast high-amplitude waves. As shown above, inclusion of the terms of the order of κ^2 into the $(h - q)_1$ model creates the effect of smoothing the leading fronts, which is most noticeable for highly viscous liquids.

In Fig. 5 we have compared the wave profiles for $\delta = 0.1$ and $\gamma = 3370$ and various wavenumbers α. From the calculations it can be seen the formation of fine-scale ripples as a result of a sequence of bifurcations ahead of the wave front of maximum amplitude. In Fig. 5 we have compared the wave profiles at $\delta = 0.1$ and $\alpha = 0.25$ for liquids with various Kapitsa numbers. There are no ripples for small γ.

4. FROM PERIODIC SOLITARY WAVES TO SOLITONS

As the wavenumber α tends to zero, the periodic solutions of the system of evolutionary equations go over into solitons, i.e., regular solitary waves. In the steady-state regime of the wave traveling at the veloc-
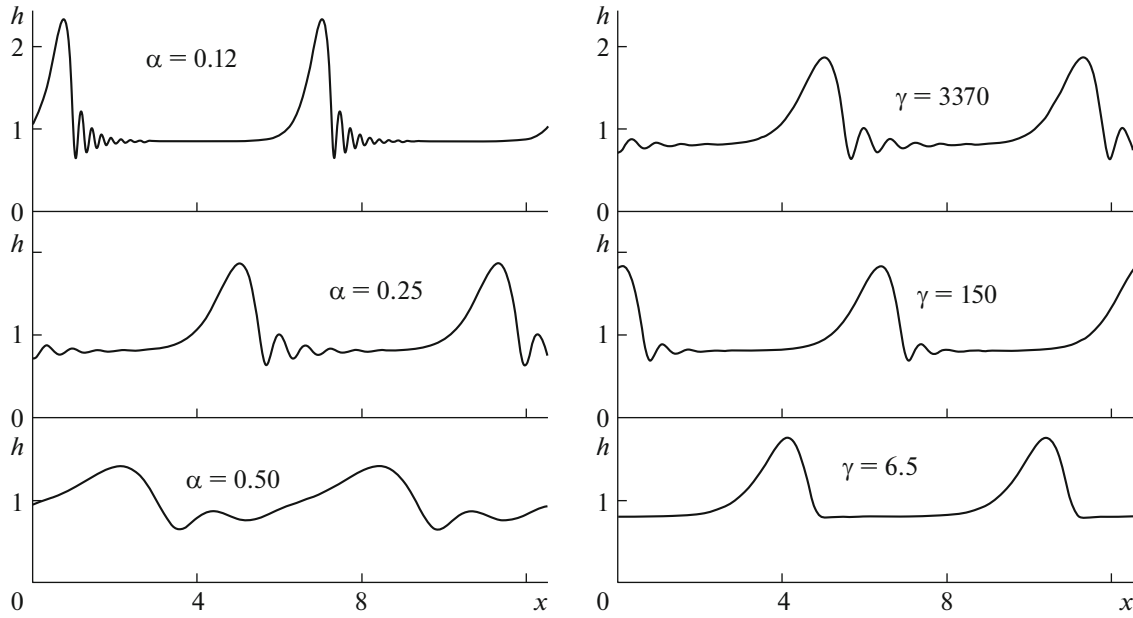
Fig. 5. Shapes of the wave profile for various wavenumbers α and Kapitsa numbers γ.

ity c we have $q_x = ch_x$. Eliminating the flow rate q from the system of equations, we can obtain the following third-order equation for the film thickness h:

$$h^3 h_{xxx} + \delta[6(1-c) - c^2 h^2]h_x + h^3 - 1 + c(1-h),$$
$$- \kappa^2 \left(\frac{7}{12} ch_{xx} h^2 + \frac{9}{4}(1-c)h_{xx} h - \frac{3}{2}(1-c)h_x^2 \right) = 0. \tag{4.1}$$

In this case the boundary conditions will be as follows:

$$x \to \pm\infty: \quad h \to 1, \quad h_x, h_{xx} \to 0.$$

For small perturbations of the shape of film surface $h = 1 + h'$ we have the linearized equation

$$h'_{xxx} + \delta(5c^2 - 12c + 6)h'_x + (3 - c)h' - \kappa^2\left(\frac{9}{4} - \frac{5}{3}c\right)h'_{xxx} = 0.$$

We will consider the perturbations of the form $h'(\eta) = \hat{h}\exp(\sigma\eta)$, where $\hat{h}$ is the perturbation amplitude and $\eta = x - ct + x_0$. Then we obtain the following dispersion relation:

$$\sigma^3 + \kappa^2\left(\frac{5}{3}c - \frac{9}{4}\right)\sigma^2 + \delta(5c^2 - 12c + 6)\sigma + 3 - c = 0.$$

The solution of this equation is three roots, one of them is real and two roots are conjugate complex. In the case of positive solitons (when $c > 3$) we have

$$\sigma_1 > 0, \quad \sigma_{2,3} = a \pm ib, \quad a < 0.$$

In this case the asymptotic behavior of the rear and leading fronts of a traveling solitary wave (soliton) as $\eta \to \mp\infty$ is given by the formulas

$$h = 1 + A\exp\sigma_1\eta, \quad \eta \to -\infty,$$
$$h = 1 + B\exp a\eta \sin b\eta, \quad \eta \to \infty, \tag{4.2}$$
$$\eta = x - ct + x_0, \quad A, B, x_0 \text{ are constants.}$$

For $\kappa^2 \ll 1$ the wave solutions of the model $(h - q)$ system of study [2] are characterized by the presence of capillary ripples on the leading front of fast high-amplitude waves of the type of solitary waves and solitons. Inclusion of the terms of the order of κ^2 into the $(h - q)_1$ model creates the effect of smoothing of the leading fronts which is in agreement with the experimental observations of waves, in particular, in highly
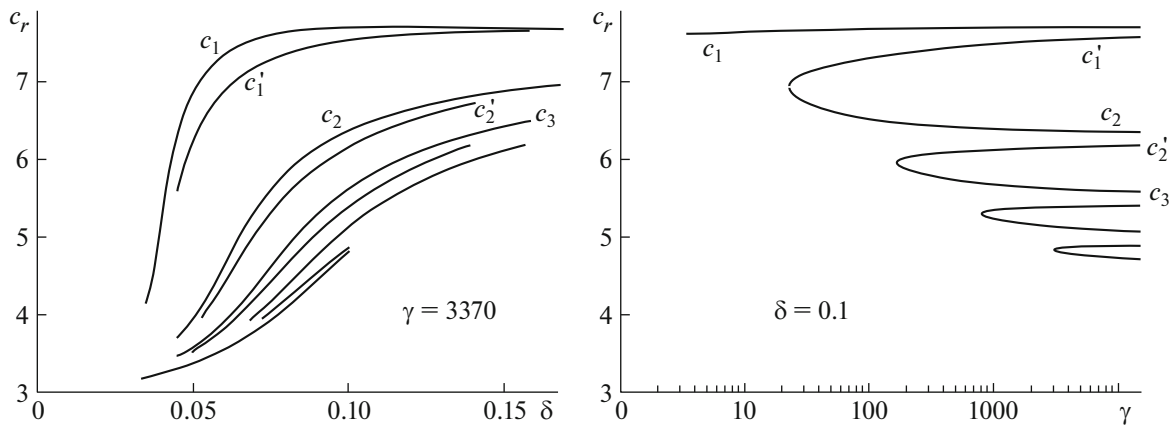
Fig. 6. Domains of existence of positive solitons for the model $(h - q)_1$ system.

viscous liquids. As the pair of regime parameters γ and κ approaches the bifurcation saddle-point curve, on the leading wave front the capillary ripple amplitude decreases rapidly. For example, for $\delta = 0.15$ and $c = 4$, as the Kapitsa number decreases from $\gamma = 3750$ to $\gamma = 3.572$ (Table 1), the exponent factor $a < 0$, that ensures damping of the ripple wave amplitude as $\eta \to \infty$, increases in absolute value in $11-16$ times. At the same time, the ripple wave length increases twice and the shape of the rear front remains almost the same.

For the single-parameter $(h - q)$ model system the domain of existence of positive solitons represents a denumerable set of intervals outside which there are no solutions. In the case of using the two-parameter $(h - q)_1$ model system the number of these intervals becomes finite for given bounded values of the Kapitsa number γ. For example (see Fig. 6), for $\delta = 0.1$ and $\gamma = 3370$ their number is equal to five, while for $\delta = 0.1$ and $\gamma = 160$ we have two intervals. For $\delta = 0.1$ and $\gamma < 22.8$ there exist no finite intervals inside which there are no bounded solutions of the problem.

In Fig. 7 we have reproduced the shapes and the phase portraits of a positive double-humped soliton C_1' for $\delta = 0.1$ and the Kapitsa numbers $\gamma = 3370$ and $\gamma = 6.5$. As in the case of regular periodic waves, decrease in the Kapitsa number for highly viscous liquids and the corresponding increase in the parameter κ leads to smoothing the oscillations on the leading front of soliton, while the shape of the rear part varies only slightly.

In Figs. 8 and 9 we have compared the results of the present calculations and the experimental data for various liquid film flow regimes.

In Fig. 8 we have reproduced the data of a series of experiments [13] in the case of highly viscous liquids (domain B in Fig. 1) over the range of Kapitsa numbers γ from 2 to 130. The calculations carried out for $\gamma = 6.5$ and in the optimum regime (maximum mean flow rate $q_{0\max}$) showed that good agreement of the dependence of the maximum wave amplitude $h_{\max}$ on the dimensionless Weber number We can be observed in the domain We > 0.1.

In [18] a comparative analysis of the methods of calculations of nonlinear waves formed in film during the spatial and temporal development of perturbations of the main steady-state flow was carried out on the base of using the similarity transforms. The use of invariant properties of evolutionary equations made it possible to compare the properties of wave regimes and the obtained characteristics of regular waves with the data of numerical solution of the corresponding spatial boundary-value problem [19], including the shape of the wave of appearing film flow.

In [20] the extended boundary element method was used to solve the system of Navier–Stokes equations numerically. In that study good agreement between the obtained characteristics of limiting wave regimes and the data [18] for the optimum regime of the set of dominating waves, namely, the global attractor, was demonstrated.

Next numerical investigations of film flows were carried out in the regimes of constant flow rate $q_0 = 1$ [18].

In Fig. 9a we have reproduced the results of calculations for a thin film of highly viscous liquid for $\delta = 0.0202$ and $\gamma = 5.9$. In [21] the experimental data were given for liquid film flow at Re $= 0.5$. The calcu-
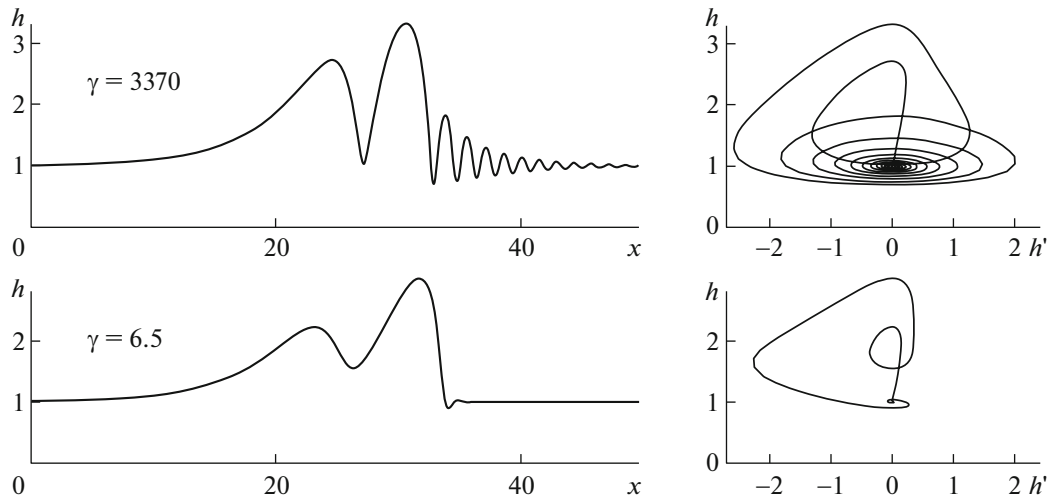
Fig. 7. Shapes and phase portraits of the positive two-humped soliton C_1' for $\delta = 0.1$.
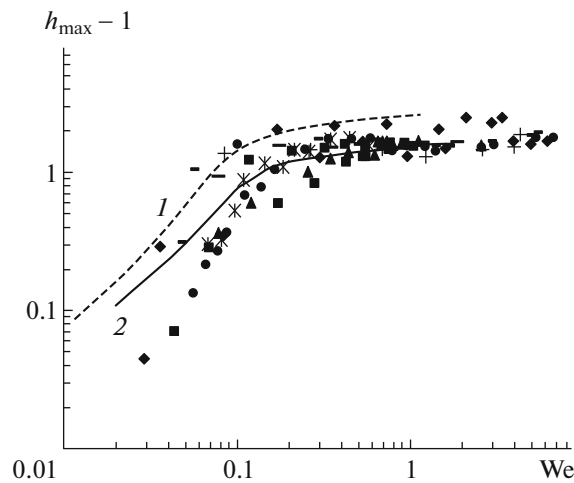

Fig. 8. Comparison of the calculation results ($\gamma = 6.5$) with the experimental data [13]: curve 1 corresponds to the dependence of $h_{max} - 1$ on We for the maximum phase velocity c_{rmax}; curve 2 corresponds to the dependence of $h_{max} - 1$ on We for the maximum mean flow rate q_{0max} (optimum regime [2]); dots note the data of a series of experiments [13] over the Kapitsa number range $2 < \gamma < 130$.

lations carried out in the present study are given for a thin layer of highly viscous liquid ($\delta = 0.0202$ and $\gamma = 5.9$) in the (h_{max}, α), (h_{min}, α) plane. In the neighborhood of neutral curve the calculation data demonstrate good agreement of the values of the maximum and minimum film thicknesses h_{max} and h_{min} at a given wavenumber α.

In Fig. 9b we have plotted the projections of the global attractor in the (h_{max}, α), (h_{min}, α) plane for the case of a film of large thickness ($\delta = 2.75$ and $\gamma = 200$). In this case the differences of h_{max} with the experimental data [13] are not greater than $7-10\%$.

5. BIFURCATION OF THE WAVE STRUCTURES OF A HIGHLY VISCOUS LIQUID AT SMALL WAVENUMBERS (INVERSE BIFURCATION)

In the limit, as the wavenumber decreases, regular periodic wave goes over in a solitary wave. In this case, oscillations on the leading front arise and strengthen for fast solutions of equations and the number of local maxima increases. Increase in viscosity leads to smoothing these oscillations and reducing the
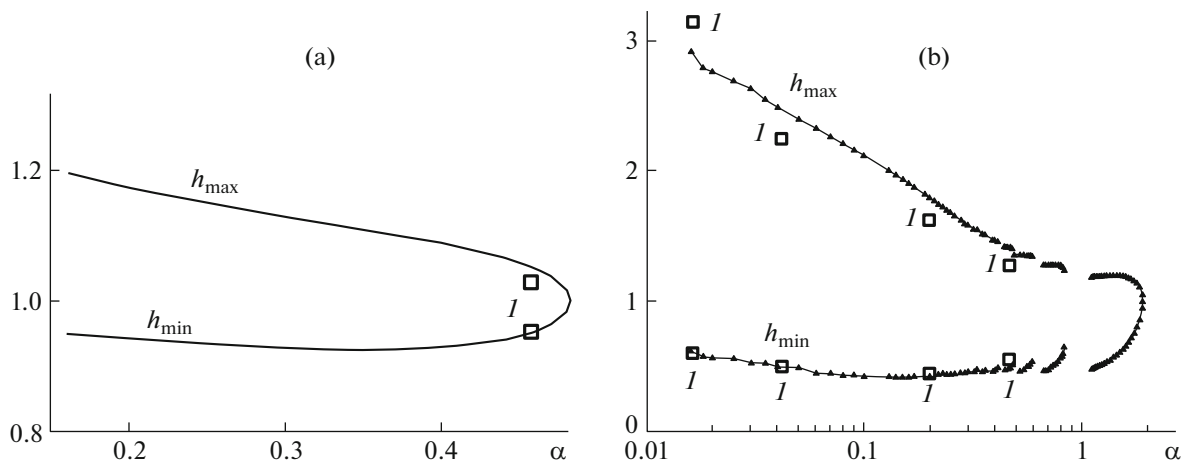
Fig. 9. Comparison of the calculation results and the experimental data: (a) projections of the global attractor for a thin layer of highly viscous liquid ($\delta = 0.0202$ and $\gamma = 5.9$) to the (h_{max}, α), (h_{min}, α) plane, 1 correspond to the experimental data [21]; (b) projections of the global attractor to the (h_{max}, α), (h_{min}, α) plane for $\delta = 2.75$ and $\gamma = 200$, 1 correspond to the experimental data [13].

number of local maxima up to their disappearance. The direct numerical calculations of Eq. (1.5) and the boundary conditions (3.2) showed that at small Kapitsa numbers ($\gamma = 6.5$) decrease in the wavenumber and successive bifurcation of the solution does not lead to an increase in the number of local maxima but leads to disintegration of wave with formation of the corresponding amount of single-humped structures. Their characteristics coincide completely with the wave parameters with the corresponding multiple increase in the wavenumber. For example, in the case of We = 0.02 and $\gamma = 6.5$ ($\delta = 0.01336$) the "single-humped" solutions exist to $\alpha \approx 0.09$. At the smaller wavenumbers we can observe the formation of two wave solutions identical each other which exist, respectively, to $\alpha \approx 0.045$. Further, to $\alpha \approx 0.03$, we can observe three wave solutions identical each other, etc. This result can be obtained by solving evolutionary equations (1.5) or (1.6), but with the boundary conditions that generalize the conditions (3.2)

$$h(0) = h\left(\frac{2\pi}{n}\alpha\right), \quad h_x(0) = h_x\left(\frac{2\pi}{n}\alpha\right), \quad h_{xx}(0) = h_{xx}\left(\frac{2\pi}{n}\alpha\right),$$

where n takes integer values 1, 2, 3, etc.

An analysis of the properties of global attractor shows (Fig. 10) that transition from the solution $n = 1$ to the solution $n = 2$ in the domain $\alpha \approx 0.09$ is connected with the fact that the local flow rate of the solution $n = 2$ at the point $\alpha = 0.1$ takes the maximum value $q_0 = 1.0055$, while for the solutions $n = 1$ the local flow rate $q_0 = 1.004$. Further, as the wavenumber decreases to $\alpha \approx 0.045$, the situation is repeated and transition to the solution $n = 3$ takes place.

As shown in [18], the frequency with the maximum growth rate which is close to the frequency of the optimum regime can affect the formation of wave together with the forced oscillation frequency. As a result, flow is restructured and the oscillation frequency changes. Then, as a result of some features of excitation of the frequency in the initial time interval, in carrying out the experiments it is possible that waves with multiple increase in the wave length are formed together with the wave structure at the "basic frequency." The observed "primary" and "secondary" wave flows developed as a result of multiple increase in the wavelength are represented by a united curve in the projection of the global attractor in the (c_r, h_{max}) plane (Fig. 10d). The possible solutions with multiple increase in the wavelength, represented as the solutions with the smaller wavenumbers $\alpha_2 = \alpha/2$, $\alpha_3 = \alpha/3$, etc., will have the lower phase velocity c_r and the smaller maximum film thickness h_{max} (Figs. 10a, 10b, and 10c). The limiting wavenumber at which inverse bifurcation occurs is equal to $\alpha_* = 0.09$ for $\gamma = 6.5$ and is equal to approximately $\alpha_* = 0.12$ for $\gamma = 40$. These quantities are close to the limiting wavenumber $\alpha_* = 0.14$ at which regular waves are observed in the experiments [16]. Note that at $\alpha_* = 0.09$ the growth rate coefficient αc_i for $n = 2$ is greater than αc_i for $n = 1$ by approximately 3.5 times and at this wavenumber the quantity αc_i for $n = 3$ takes its maximum value. Thus, when $\alpha < 0.09$, the solutions $n = 2$ and $n = 3$ begin to affect the formation of the

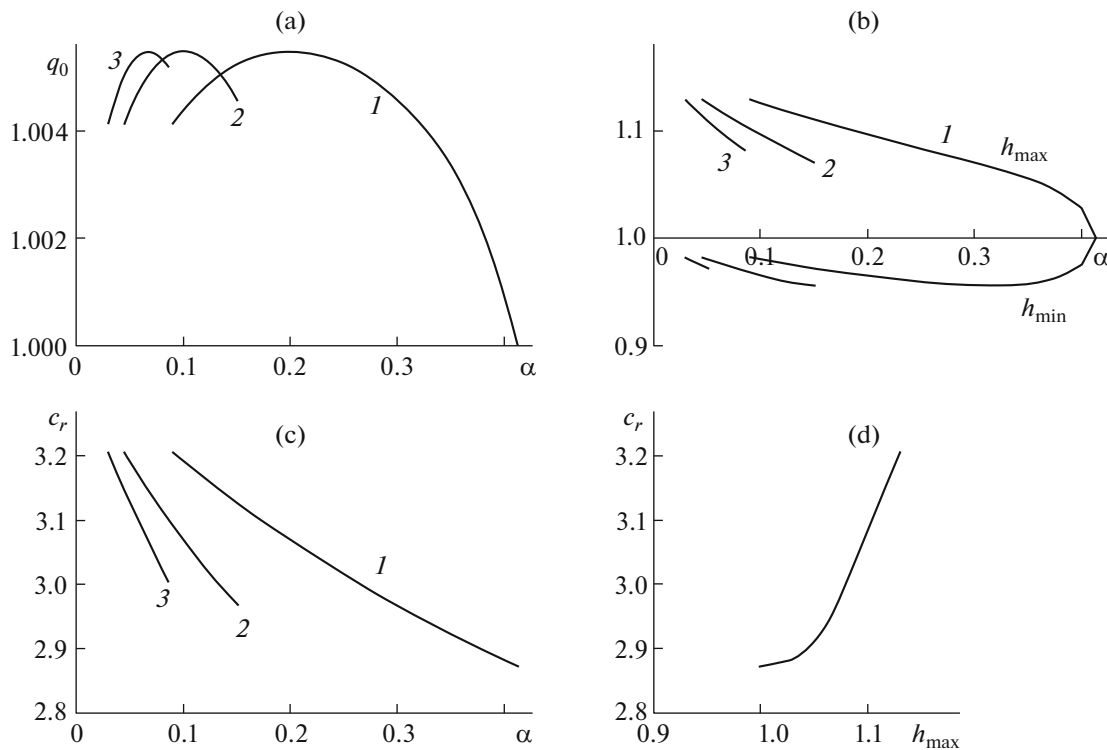**Fig. 10.** Global attractor at We = 0.02 and $\gamma = 6.5$ ($\delta = 0.01336$): (a) projection to the (q_0, α) plane; (b) projections to the (h_{max}, α) and (h_{min}, α) planes; (c) projection to the (c_r, α) plane; and (d) projection to the (c_r, h_{max}) plane.

"limiting solution" of the evolutionary system of equation. This leads to the development of "inverse bifurcation."

6. SUMMARY

The model $(h - q)_1$ system with two external parameters δ and κ that generalizes the classical $(h - q)$ model [2] with a single parameter δ to viscous liquid flows over a wide range of the Kapitsa number γ is investigated. The main dissipative terms entering into the initial boundary-value problem for the Navier-Stokes equations are conserved in the model system (1.5) of [1]. New properties of the wave solutions manifest themselves in increase in the liquid viscosity and the corresponding decrease in γ. The mechanism of suppression of fine-scale ripples and smoothing of wave fronts with decrease in γ is established. It is shown that the nature of bifurcations of nonlinear waves from the equilibrium state on neutral curve changes with decrease in γ. In the space of the regimes parameters δ and κ the curve that separates bifurcations towards slow and fast nonlinear waves is constructed. A comparison with the experimental data is carried out. It is shown that for a given δ the characteristics of regular waves formed in the spatial development can be described on the base of using the calculations of the global attractor. The phenomenon of inverse bifurcation in transition of solitary periodic waves into solitons is investigated.

FUNDING

REFERENCES

1. Shkadov, V.Ya., Two-parameter model of wave regimes of flow of viscous liquid films, *Vestnik Moskjvskogo Universiteta, Ser. 1, Matem., Mekh.*, 2013, no. 4, pp. 24−31.

2. Shkadov, V.Ya., Wave flow regimes of a thin layer of viscous fluid subject to gravity. *Fluid Dynamics,* 1967, vol. 2, no. 1, pp. 29−34.
https://doi.org/10.1007/BF01024797

3. Shkadov, V.Ya., Solitary waves in a layer of viscous liquid, *Fluid Dynamics,* 1977, vol. 12, no. 1, pp. 52−55.
https://doi.org/10.1007/BF01074624

4. Kalliadasis, S., Ruyer-Quil, C., Scheid, B., and Velarde, M.G., *Falling Liquid Films*, London: Springer, 2011.

5. Mendez, M.A., Scheid Benoit, and Buchlin, J.-M., Low Kapitza falling liquid films, *Chemical Engineering Science*, 2017, vol. 170, pp. 122−138.

6. Shkadov, V.Yu. and Demekhin, E.A., Wave motions of liquid films on the vertical surface (theory for interpretation of experiments), *Usphekhi Mekhaniki*, 2006, vol. 4, no. 2, pp. 3−65.

7. Shkadov, V.Yu., Problems of nonlinear hydrodynamic stability of layers of a viscous liquid, capillary jets, and inner flows, *Doctoral Dissertation on Physico-Mathematical Sciences, Facility of Mechanics and Mathematics of Moscow State University,* Moscow: 1973.

8. Koulago, A.E. and Parseghian, D., A propos d'une équation de la dynamique ondulatoire dans les films liquids, *Journal de Phisique,* III, France, 1995, vol. 5, pp. 309−312.

9. Nepomnyashchii, A.A., Stability of wavy conditions in a film flowing down an inclined plane, *Fluid Dynamics,* 1974, vol. 9, no.3, pp. 354−359.
https://doi.org/10.1007/BF01025515

10. Nepomnyashchii, A.A., Stability of wavy conditions in a film flowing down an inclined plane, *Fluid Dynamics,* 1974, vol. 9, no.3, pp. 354−359.
https://doi.org/10.1007/BF01025515

11. Bunov, A.V., Demekhin, E.A., and Shkadov, V.Ya., On the nonuniqueness of nonlinear wave regimes in a viscous layer, *Prikl. Mat. Mekh.*, 1984, vol. 48, no. 4, pp. 691−696.

12. Nguyen, L.T. and Balakotaiah, V., Modeling and experimental studies of wave evolution on free falling viscous films, *Phys. Fluids*, 2000, vol. 12, no. 9, pp. 2236−2256.

13. Meza, C.E. and Balakotaiah, V., Modeling and experimental studies of large amplitude waveson vertically falling films, *Chemical Engineering Science*, 2008, vol. 63, pp. 4704−4734.

14. Ruyer-Quil, C. and Manneville, P., Further accuracy and convergence results on the modeling of flows down inclined planes by weighted-residual approximations, *Phys. Fluids*, 2002, vol. 14, pp. 170−183.

15. Kapitsa, P.L. and Kapitsa, S.P., Wave flow of thin layers of a viscous liquid, *Zh. Eksp. Teor. Fiz.*, 1949, vol. 19, no. 2, pp. 105−120.

16. Alekseenko, S.V., Nakoryakov, V.E., and Pokusaev, B.T., *Volnovoe techenie plenok zhidkosti* (Wave Flow of Liquid Films), Novosibirsk: Nauka, 1992.

17. Sisoev, G.M. and Shkadov, V.Yu., Development of dominating waves from small disturbances in falling viscous-liquid films, *Fluid Dynamics,* 1997, vol. 32, no. 6, pp. 784−792.
https://doi.org/10.1007/BF03374534

18. Beloglazkin, A.N., Shkadov, V.Ya., and Kulago, A.E., Limiting wave regimes during the spatial and temporal development of disturbances in falling liquid films, *Moscow University Mechanics Bulletin,* 2019, vol. 74, no. 3, pp. 69−73.

19. Nosoko, T. and Miyara, A., The evolution and subsequent dynamics of waves on a vertically falling liquid film, *Phys. Fluids*, 2004, vol. 16, no. 4, pp. 1118−1126.
https://doi.org/10.1063/1.1650840

20. Aleksyuk, A.I., and Shkadov, V.Ya., A study of transient flows with interfaces using numerical solution of Navier−Stokes equations, *Fluid Dynamics,* 2020, vol. 55, no. 3, pp. 314−322.
https://doi.org/10.1134/S0015462820030015

21. Panga, M.K.R., Mudunuri, R.R., and Balakotaiah, V., Long-wavelength equation for vertically falling films, *Phys. Rev. E*, 2005, vol. 71, p. 036310.

Translated by E.A. Pushkar